



**HAL**  
open science

# OpenCL FPGA Optimization guided by memory accesses and roofline model analysis applied to tomography acceleration

Daouda Diakite, Nicolas Gac, Maxime Martelli

## ► To cite this version:

Daouda Diakite, Nicolas Gac, Maxime Martelli. OpenCL FPGA Optimization guided by memory accesses and roofline model analysis applied to tomography acceleration. 30th international conference on field programmable logic and applications (FPL), Aug 2021, Dresden, Germany. hal-03226257v1

**HAL Id: hal-03226257**

**<https://hal.science/hal-03226257v1>**

Submitted on 20 May 2021 (v1), last revised 14 Oct 2021 (v2)

**HAL** is a multi-disciplinary open access archive for the deposit and dissemination of scientific research documents, whether they are published or not. The documents may come from teaching and research institutions in France or abroad, or from public or private research centers.

L'archive ouverte pluridisciplinaire **HAL**, est destinée au dépôt et à la diffusion de documents scientifiques de niveau recherche, publiés ou non, émanant des établissements d'enseignement et de recherche français ou étrangers, des laboratoires publics ou privés.

# OpenCL FPGA Optimization guided by memory accesses and roofline model analysis applied to tomography acceleration

Daouda Diakite<sup>1</sup>, Nicolas Gac<sup>1</sup>, Maxime Martelli<sup>2</sup>

<sup>1</sup> Université Paris-Saclay, CNRS, CentraleSupélec, L2S, 91190, Gif-sur-Yvette, France.

<sup>2</sup> Information Services Group, Inc.

**Abstract**—Backward projection is one of the most time-consuming steps in method-based iterative reconstruction computed tomography. The 3D back-projection memory access pattern is potentially enough regular to exploit efficiently the computation power of acceleration boards based on GPU or FPGA. The high-level tools like HLS or OpenCL ease consider such particular memory accesses during the design flow without specific hardware IPs. This paper proposes an OpenCL acceleration of the voxel-driven 3D back-projection algorithm on an Arria 10 FPGA. This design flow is based initially on an offline memory access analysis, then iteratively on a performance analysis of each new implementation represented on a Berkeley Roofline model.

By taking advantage of the FPGAs local memory architecture, we have succeeded to design an efficient pipeline reaching maximum bandwidth with stall-free access underlining this platform's interest for memory optimization. Our design flow allowed for a significant improvement of our initial algorithm's computational intensity, resulting in better performance on FPGA. It reaches comparable performance to an embedded GPU implementation and other computed tomography algorithms on FPGAs.

**Index Terms**—FPGA, HLS, memory access analysis, roofline model, tomography reconstruction

## I. INTRODUCTION

X-ray computed tomography(CT) is an imaging technique that initially found its application in the medical field. It has been extended to industrial applications such as non-invasive human body investigation and non-destructive testing of industrial materials. Model-Based Iterative Reconstruction (MBIR) algorithms are proved to produce better image quality at the cost of expensive computational time. To reduce the reconstruction time of CT algorithms, hardware accelerators are required. For the past few years, GPUs have been the preferred architecture due to their massively parallel computing pattern. However, FPGAs can be re-considered thanks to their low latency, power efficiency, and accessibility through High-Level Synthesis (HLS) tools provided by leading manufacturers like Intel or Xilinx.

Field programmable gate arrays (FPGAs) based on HLS tools are experiencing great consideration as an

acceleration platform for many applications such as high-performance computing [1], [2], [3], deep neural networks [4], [5]. The maturity of their architectures and many built-in floating-point units (DSPs) in the latest FPGAs explain this interest. These floating-point units provide high design flexibility and are optimized to support high-performance DSP applications in IEEE 754 compliant floating-point single precision. For instance, Intel Stratix 10 [6] and Intel Agilex [7] devices can achieve up to 9 TFLOPS and 20 TFLOPS respectively. Unlike CPUs and GPUs, FPGAs can express spatial and temporal (fine/coarse-grained) parallelism, making them suitable for algorithms with sequential patterns and high data dependency. In the past, these various parallelisms are extracted for tomography through the HDL languages requiring a basic knowledge of hardware [8], [9], [10], [11]. This level of abstraction can be heavy and time-consuming development based on the complexity of specific algorithms. Hence, the emergence of tools with a high level of abstraction allows a broader audience to use FPGAs through software programming languages like C, C++, or OpenCL. FPGAs with HLS have recently been subject of evaluation in computed tomography algorithms such as Maximum Likelihood Expectation Maximization [12], [13], 3D back-projection [14], [15] or CT data alignment in memory [16]. These work focus on FPGA specific optimization for computed tomography in algorithm architecture co-design purpose. However, other works have based their optimization on the algorithm itself. Choi et al. [17] proposed a Ray-driven voxel-tile parallel approach hence take advantage of FPGA BRAM blocks and the data reuse rate. Zhang et al. [18] also proposed a parallel beam-based reconstruction on FPGA to exploit on-chip BRAM intensively.

To address the memory access for intensive algorithm, Intel FPGA SDK for OpenCL [19], besides multiple memory models, proposes multiples load store unit (LSU) based on the memory access pattern. The compiler implements the LSU that best matches the kernel memory invocation. However, the programmer needs to help the AOC compiler in the code writing to choose adequate LSU as discussed in [20]. FPGAs DRAM bandwidths are typically insuffi-

cient to meet memory-bound applications. Nevertheless, available block RAM (BRAM) can be an alternative to achieve maximum throughput. Although, these BRAM are very small in size for applications with huge data such as computed tomography. A data access strategy must be developed to take advantage of these on-chip blocks without stalling the pipeline.

In this paper, we propose an OpenCL acceleration of the voxel-driven 3D back-projection algorithm on an Arria 10 FPGA. This design flow is initially based on an offline memory access analysis then iteratively on a performance analysis represented on a Berkeley Roofline [21]. Our implementation is based on blocks of voxels reconstruction taking into account the data reuse rate, and exploiting the local memory on FPGA using Intel FPGA SDK for OpenCL. We compare the results with others FPGA implementations in terms of throughput, execution time, and design efficiency. The remainder of this paper is organized as follows: in section II we present the 3D back-projection, the acceleration platform and the offline memory analysis. We introduce in section III our OpenCL architecture of the 3D back-projector. The optimisation guided by the roofline model and experimental results are provided in section IV.

## II. BACKGROUND AND MOTIVATION

### A. 3D back-projection algorithm

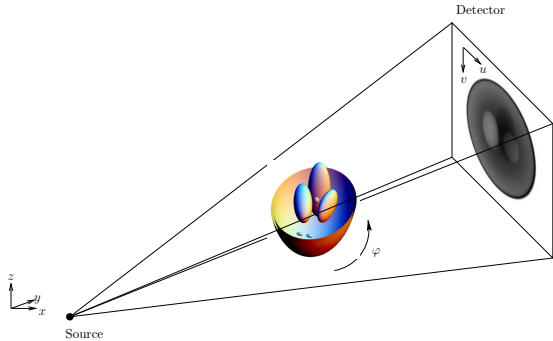


Fig. 1: X-RAY CT Projection

3D Computed Tomography (CT) aims to acquire the internal density  $d$  of 3D objects from external measurements  $S_{CT}$  called sinogram. An object (3D volume) is placed between an X-ray source and a detector plane as illustrated Fig. 1. The 3D back-projection used in iterative reconstruction and described in detail in [8] algorithm is given by:

$$d(c) = \int S_{CT}(u(\varphi, c), v(\varphi, c), \varphi) \cdot w(\varphi, c)^2 d\varphi \quad (1)$$

where  $c = (x, y, z)$  are the voxel coordinates,  $(u, v)$  are the cone beam coordinates,  $\varphi$  is the angular trajectory of the detector and  $w$  is the distance weight.

$$u(\varphi, c) = x * \cos(\varphi) + y * \sin(\varphi) \quad (2)$$

$$v(\varphi, c) = x * \sin(\sin\varphi) - y * \cos(\varphi) + z \quad (3)$$

For each voxel  $(x, y, z)$ , the projection of its contribution is located at a position  $(u(x, y, \varphi), v(x, y, z, \varphi))$  on the detector. The contribution on the detector is computed by bi-linear interpolation. In our design, the interpolation is replaced by the nearest neighbor method to reduce resource consumption and computation overhead.

### B. Acceleration platform

OpenCL is an open-source parallel programming API for heterogeneous processing platform (CPU, GPU, FPGA...). Based on the C99 standard, OpenCL supports both data and task-parallel programming models (Single Work-Item Kernel and NDRange Kernel) [22]. An OpenCL application is composed of two programs: a host application and the kernel compiled separately using Just In Time (JIT). The JIT compilation is not supported due to the long-time place and route step for bitstream generation on FPGAs. Therefore the OpenCL kernel is compiled offline using a vendor-specific compiler since FPGA does not support JIT compilation due to the place and route step in the synthesis flow. The Board Support Package (BSP) as shown in Fig. 2, provided by the board manufacturers, allows programmers to run the kernel executable on the target FPGA. It packages features such as IP Cores, DDR controller, PCIe controller, and DMA drivers to establish communication between the host and the FPGA device. Many Intel FPGA manufacturers provide FPGA with their BSP to quickly design and run Intel devices applications using Intel FPGA SDK for OpenCL. Intel FPGA SDK also provides, besides OpenCL directives, many FPGA-specific optimizations to fully harness the device potential.

These compilers implement different optimization based on their particular intermediate representation (IR), such as pipelining or expressing data-level parallelism. However, they suffer from a lack of support for many other unexploited FPGA-specific optimizations for arithmetic operations [23] for instance. Hence, harnessing FPGAs' full potential via HLS tools requires knowledge of their architecture and a significant effort to adapt the application because it is not performance-portable. This leads to the evaluation of OpenCL optimization techniques on FPGA by various works [2], [15], [24], [1].

### C. Offline Memory Access Analysis

The global memory access on Intel FPGA, despite its high latency, can be efficient for contiguous and repetitive memory accesses thanks to automatic embedded on-chip cache implementations in Load-Store Units (LSUs). For non-sequential and random accesses, these automatic caches, inferred by the Intel compiler, will be much less relevant to speed up the application on FPGAs efficiently. Their inference will be counterproductive and waste valuable BRAM resources with a high risk of memory stalling. Such behavior is confirmed in the 3D back-projection

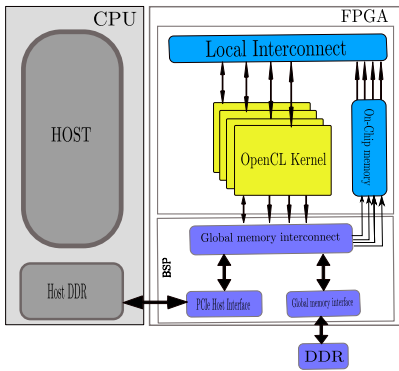


Fig. 2: Intel FPGA SDK for OpenCL platform

algorithm by [14], and many CT algorithms, so their acceleration on FPGAs remains a big concern. An offline study of the algorithm memory access pattern is required to either make it regular or prefetching sinogram data to the on-chip BRAM before performing voxel reconstruction. Prefetching sinogram contribution to reconstructing one voxel is not efficient and leads to more DRAM transactions. Therefore with the highest data reuse rate, maximum computation is performed at the BRAM level to take advantage of the local memory.

Since the whole projection data cannot fit in FPGA on-chip memory, block of voxels reconstruction will be wise to perform this task and overcome the problems mentioned above efficiently. The projection of a 2D or 3D block of voxels corresponds to a rectangle shape in the detector plane for a given projection angle  $\varphi_i$ . A high data re-utilization exists and is even more important for neighboring voxels. For a  $\varphi_i$ , voxels in the same block will contribute to the detector plane in the same zone. The main concern is to capture the sinogram footprint without loss of information and calculate the coordinates of its boundary. For each voxel  $(x, y, z)$ , its reconstruction depends on its  $\phi$  angular projections, these projections are spatially distant due to their storage in the sinogram following the order  $(u, v, \varphi)$ . To increase the spatial locality, reconstruction by a group of voxels in the same block is beneficial. Instead of looking for the contribution of a single voxel in the sinogram data for a given projection angle, one could look for the contribution of all the voxels in the block, which will always be in the same memory zone thanks to the CT system geometry. This makes access to memory contiguous and regular to either take advantage of the cache or prefetch the data in local memory itself. With prefetch, we use the BRAMs memory extensively with access latency reduced to one cycle, and automatic caching is avoided.

The sinogram footprint for a block is dependent to the shape of block of voxels. For a block of size  $(B_x, B_y, B_z)$ , the 2D rectangle coordinates of the projection shape  $(local_u, local_v)$  depends on  $B_x$ ,  $B_y$ , and  $B_z$  such as:

$local_v = \sqrt{B_x^2 + B_y^2}$  as pointed out in [15] and  $local_v = \sqrt{2} * B_z$ . The data reuse rate is computed by the following formula and illustrated in Fig. 3.

$Data\ reuse = \frac{B_x * B_y * B_z}{\#Memory\ access\ I/O}$  where the  $\#Memory\ access\ I/O$  is obtained by a static analysis of the CPU code.

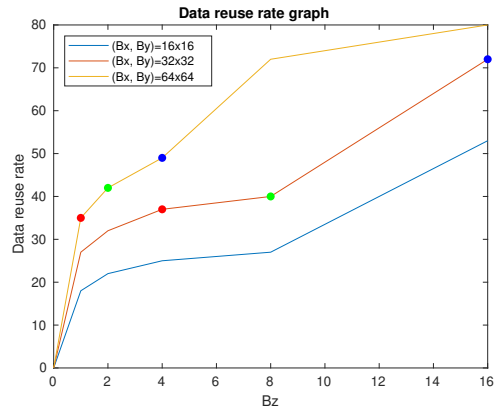


Fig. 3: Data reuse rate

The reuse rate is shown in Fig. 3 with different block sizes, same colored dots match the same number of voxels in the block, i.e. the same BRAM consumption. This allows us to see the effect of block shape and size that provides the best reuse rate. In our case, we chose  $B_x$  and  $B_y$  equals and vary  $B_z$  in the axial direction. We notice that we have best reuse rate from  $B_z = 8$  and higher. The  $64 \times 64 \times 8$  block shape gives the best trade-off between reuse rate and BRAM consumption. It uses fewer BRAM resources and required fewer projections data to prefetch for approximately the same reuse rate as the  $64 \times 64 \times 16$  shape.

### III. HARDWARE IMPLEMENTATION

3D back-projection is one of the most time-consuming steps in iterative reconstruction. In our architecture we use on-chip memory to leverage the BRAM bandwidth and therefore decrease the global memory bandwidth.

#### A. FPGA BRAM memory

FPGA local memory does not support cache hierarchy but has some characteristics for implementing dedicated on chip memory blocks. Accesses to local memory are mapped to a physical port, to avoid access conflict, one should infer the required number of read/write ports or replicate local memory to have a stall-free configuration. For pipeline efficiency, Intel compiler creates private copies to enable concurrence execution of multiple loop iterations. Increasing number of private copies consumes more memory resources but and at the same time maximize the bandwidth and increase the occupancy of the compute unit. A trade-off must be made between performance and the BRAM resources consumption.

## B. Architecture of the back-projector and Scalability

The 3D back-projector is memory-bound which could result in catastrophic performance on FPGA. Its memory access pattern is not cache friendly, and the HLS compiler would infer automatic caches to take advantage of data redundancy and improve performance. This led to two significant problems: because the FPGA caches are not as perfect as CPU or GPU ones, the cache misses are very penalizing. Hence using Intel automatic cache became a lock when optimizations such as loop unrolling were applied in the case of algorithm 1 for instance. Loop unrolling consists of fully or partially replicating the loop body and increasing the BRAM usage, thus preventing DSPs' maximum use. Our new implementation does not require the Intel automatic cache. Instead, we use the dedicated BRAM to prefetch all the data needed to accumulate multiple voxels intensities for one angle view. The challenge of using on-chip memory is that all access must be stall-free with no arbitration. For this purpose, banking and replication of local memory to support multiples access are necessary. The Intel FPGA SDK has the attributes necessary to control the local memory depth, bank, and read/write ports.

---

### Algorithm 1 Kernel OpenCL for BP-cache

---

```

for all  $z_n, y_n, x_n$  do
   $voxel_{sum} \leftarrow 0$ 
  #pragma unroll 32
  for all  $\varphi$  do
     $Compute(u_n, v_n)$ 
     $voxel_{sum} += sinogram[u_n, v_n, \varphi]$ 
  end for
   $volume[x_n, y_n, z_n] = voxel_{sum}$ 
end for

```

---



---

### Algorithm 2 Kernel OpenCL for BP-prefetch

---

```

for all  $block_{z,y,x}$  do
  for all  $\varphi$  do
     $Compute(u_0, v_0)$ 
     $Pretching\ sinogram\ data$ 
    #pragma unroll 64
    for all  $z_n, y_n, x_n \in block_{z,y,x}$  do
       $voxel_{sum} \leftarrow 0$ 
       $Compute(u_n, v_n)$ 
       $block[z_n, y_n, x_n] += sino\_local[u_n, v_n]$ 
    end for
  end for
   $volume[z_n, y_n, x_n] \leftarrow block$ 
end for

```

---

In our new implementation (algorithm 2), the critical path consists of reconstructing the block of voxels with the innermost loop over the voxels. The loop body, considered as processing element (PE), can be replicated for parallel

voxel intensity computation by loop unrolling. It is then possible to have 64 PEs (see Fig. 4) in our architecture without exceeding available resources. Each PE must have free access to local memory, which requires a physical port for each memory read. If there is not enough port, the memory requests will be made with arbitration which will cause a severe performance problem of the pipeline by increasing the Initiation Interval (II) [25]. The architecture's input is the image projections in the detector plane as in Fig. 4. For each projection angle  $\varphi_i$ , we prefetch all contributions required (red rectangle) for the voxels accumulation in the block. We load more memory data than required to assure correct reconstruction and take advantage of memory coalescence. After the accumulation over all projections angle  $\varphi_i$ , the reconstructed block of voxels (blue cube) is written back to the global memory volume.

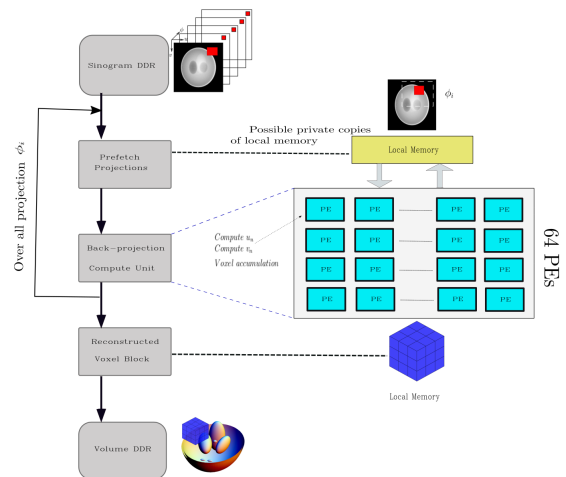


Fig. 4: The proposed architecture with 64 PEs. Each PE has a free access to read local memory, and is responsible for one voxel update at the time.

Our architecture requires 64 reads port (32 bits wide) for all the PEs to read sinogram data in local memory, and 2 read/write ports (2048 bits wide) for accumulation in the block of voxels. Intel recommends to have four or less read/write ports to local memory for stall-free access without arbitration [25]. We have a total memory replication factor of 22 to support parallel access to the local sinogram. Each replicate has the same sinogram data for the reconstruction. In addition, we place 8 privates copies of the local memory for concurrent execution of loop iterations ( $\varphi$  loop in algorithm 2). This reduces the overall latency, and increases the pipeline efficiency.

## IV. ROOFLINE ANALYSIS AND RESULTS

The Berkeley Roofline model was used to highlight the optimization steps after improving our implementation's computational intensity. We first build our architecture to



determine the attainable performance and then tuning the block size for better performance.

### A. Experiment setup

In this experiment we do not consider the data transfer between the host and the device therefore the considered run-times do not include memory transfer. However, to speed up the memory transfer, the allocate data must be at least 64 bytes aligned to allow the Direct Memory Access (DMA). To allocate an aligned memory, the posix function `posix_memalign` can be used in the host side. In our experience the aligned memory achieves better transfer rate than non-aligned in all cases. We used for this work the FPGA FLIK Arria 10 device, which comes with 8 GB of DDR4-2133 memory, with a maximum frequency of 480 MHz. The FPGA is connected in PCIe connection (via Thunderbolt 3) to the host system. The considered volume is a  $256^3$  voxel, with 256 angles variations. Each kernel execution is monitored through the Intel FPGA dynamic Profiler for OpenCL. For each kernel, this tool provides, amongst other things, the operating frequency, the execution time, the logic utilization, and the latency, bandwidth, and stall of most memory access.

### B. Roofline model for FPGAs

The roofline model first introduced by [21] is a tool for visually and quickly observing the possible limitations of an algorithm relative to theoretical maximum performance on a target architecture. The model is characterised by two keys parameters which defines two roofs: the device peak performance and the attainable bandwidth. The work of Williams et al. [21], focused on CPU multi-core architectures, was extended to the FPGA architectures in [26] through HLS tools and taking into account the resource utilization of the device. For FPGAs, the model is architecture-dependent and application-dependent, so they introduced the scalability parameter determined by the available resources on the target FPGA for pipeline replication. The scalability gives us an indication of the replication potential of the elementary pipeline. The paradigm on FPGA is even more complex, the theoretical limits provided by vendors are far from those obtained after synthesis. To collect data, we need to use the profiling tools available, which allows us to have more design information such as adequate bandwidth, operating frequency, and runtime.

We use the roofline model to iteratively analyze our algorithm and guide the optimizations. Each algorithm results on a specific roofline for FPGAs. The performance roof is determined by the number of resources consumed and the effective operating frequency. The dynamic profiler gives the actual DRAM bandwidth achieved. Table I lists the number of operations GBOP and the number of memory accesses of the 3D back-projection in GB. We determine the Computational Intensity (CI) for different versions of the algorithm. The implementation with

automatic cache is memory-bound (see Fig. 5 red dot) due to the lack of spatial and temporal data locality in the sinogram. The computational intensity of this version very low, elaborating another strategy to access off-chip memory might substantially increase the CI and allow the use of more DSP slices to improve the performance.

	$B_z$	Operations GBOP	DRAM (GB)	CI
BP-cache	N/A	236	17.2	13.7
BP-prefetch	1	253	1.1	236
	2	253	0.8	314
	4	253	0.67	377
	8	253	0.6	419
	16	253	0.57	443

TABLE I: Roofline analysis Memory and Operations

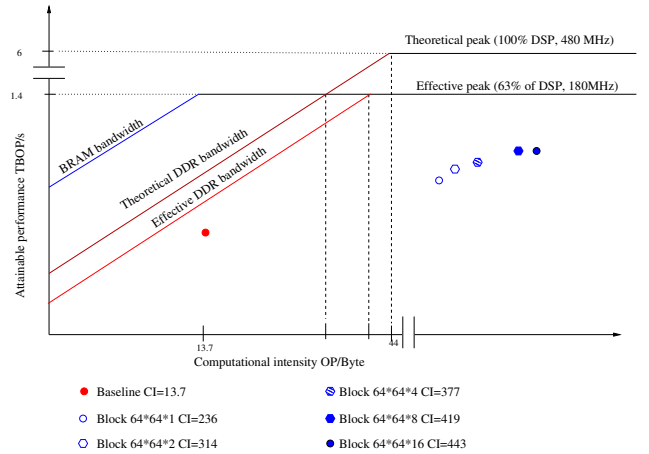


Fig. 5: Roofline of 3D back-projection with different  $B_z$

The algorithm memory access pattern has changed, global memory invocation is now contiguous and considerably reduced, hence the bandwidth is under good use. We can see that CI increases as long as the block size grows until it reaches the maximum data reuse rate. The memory operations in the table I take into account memory coalescence allowed by loop unrolling.

### C. Effect block size variation

Version	BRAM (%)	DSP %	Stall (%)	Occ (%)	Freq (Mhz)	Time (s)	
BP-Cache	72	27	71.27	24.6	150	3.65	
BP-Prefetch	$32^2 \times 1$	50	58	88.34	12.3	197	2.78
	$32^2 \times 2$	50	58	90.1	24.3	190	1.46
	$32^2 \times 4$	50	58	7.22	43.5	195	0.893
	$32^2 \times 8$	50	58	0.44	60.3	180	0.719
	$64^2 \times 1$	50	63	2.79	43.5	183	0.843
	$64^2 \times 2$	50	63	0.34	58.9	186	0.658
	$64^2 \times 4$	50	63	0.2	74.4	187	0.529
	$64^2 \times 8$	62	63	0.06	84.1	188	0.425

TABLE II: Block size variation effect on the performance

Table II shows the results of our implementation, the BP-cache design is an optimized version of the 3D back-projection using burst-coalesced cached LSU (algorithm

1). OpenCL optimizations such as loop pipelining, loop unrolling were applied to this version to accelerate the reconstruction time. This version suffers from a high pipeline stall percentage because of the memory access pattern making the global bandwidth the main bottleneck. The implementations based on blocks of voxels (algorithm 2) using BRAM memory achieve better performance compared to the BP-cache version. The table II shows the effect of block shape and size variation. We saw in Fig. 3 that high reuse rate is achieved when there is many voxels in the block. For  $B_x$  and  $B_y$  set to 32, we need to increase  $B_z$  to maximize the number of voxels. For instance, the blocks  $64 \times 64 \times 1$  and  $32 \times 32 \times 4$  have the same number of voxels and approximately the same reuse rate. However, the reconstruction based on the  $64 \times 64 \times 1$  block is faster than the  $32 \times 32 \times 4$ . The memory access pattern is a bit different for the two block, due to cubic shape the stall percentage of the  $32 \times 32 \times 4$  is slightly high with lower kernel runtime. The performance for blocks with  $B_x = B_y = 64$  are always better than  $B_x = B_y = 32$  given the same number of voxels. In the design, all loops are pipelined with an Initiation Interval (II) of 1. Once  $B_x$  and  $B_y$  are fixed,  $B_z$  tuning allows to optimize the data reuse rate and therefore the overall performances as illustrated on table II.

We have obtained a better execution time with the  $64 \times 64 \times 8$  block, which corroborates the static study performed on the data reuse. The pipeline occupancy is 84.1% with a 0.06 stall percentage, which characterizes an excellent utilization of the FPGA device. Even when designing in HDL language, the purpose is to implement a pipeline with a 0% stall percentage. Compared to the previous BP-cache design, we achieved a speedup of 8.6 at 188.9MHz.

#### D. FPGA design

The resource usage of the  $64 \times 64 \times 8$  block version is presented in table III. As mentioned above our design contains 64 PEs, the overall back-projector design uses 949 DSP slices and 1952 blocks RAMs. The BRAM usage also includes the memory replication overhead to support concurrent access within the pipeline.

	FF	LUT	BRAM	DSP
Usage	407183	184616	1952	949
Available	1577720	788860	2537	1518
Ratio	25%	44%	62%	63%

TABLE III: FPGA resources consumption on Arria 10

#### E. Performance comparison

To fairly compare different implementations with different problem sizes, we use the Giga Updates Per Second (GUPS) indicator, which is insensitive to the size of the problem, by using the formula given in [27].

$$GUPS = \frac{GU}{Time_{kernel}} \quad \text{with} \quad GU = \frac{N_{voxel} * N_{acc/voxel}}{1024^3} \quad (4)$$

with  $N_{voxel}$  the size of volume and  $N_{acc/voxel}$  the number of accumulation per voxel. The GUPS in [27] use  $1024^3$  and not  $1000^3$ , so we use recalculate all GUPS according to this formula.

Our work achieved a comparable performance as our embedded GPU implementation in terms of GUPS, as shown in table IV. Hence, FPGAs are more energy-efficient than GPUs, and our FPGA implementation could potentially achieve better performance per watt (GUPS/W) than the GPU implementation. For FPGA accelerations, Vivado HLS is commonly used to achieve acceleration as in [17], [16], although we use in this work Intel FPGA SDK for OpenCL. OpenCL is a bit at a higher abstraction than HLS. Hence the designer has more control over the pipeline using HLS compilers such as Vivado HLS or Intel HLS compiler. Therefore we have achieved low GUPS than the works using HLS. However, we use much fewer resources than those works since our target device is a middle-range Intel FPGA. Choi et al. [17] used, with helical geometry, the Convey HC-1ex platform with four FPGAs running at 100 Mhz of operating frequency, and their design consumes 1408 DSP slices. Wen et al. [16] targeted the Xilinx ZCU102 platform (based on an UltraScale FPGA) with an overall DSP utilization of 1476 at 299.97 Mhz. We then evaluate all the FPGA implementations' design efficiency by comparing the Giga update perform per cycle by each MAC (Multiply ACCumulator). Our OpenCL implementation on Arria 10 has approximately the same design efficiency as the HLS ones (table IV). We evaluate our pipeline efficiency by computing the update/cycle/PE, which is equals to 0.84 ; it demonstrates that our pipeline works efficiently close to the optimal compute throughput of 1 update/cycle/PE.

Reference	Platform	Volume	Acc. /voxel	Time (s)	GUPS	GUpdate /cycle /MAC
[17]	4 × Virtex-6	$512^2 \times 372$	831	3.7	20.4	0.156
[16]	ZCU102	$1024^2 \times 128$	502	2.10	29.9	0.073
GPU	Jetson TX2	$256^3$	256	0.25	15.8	0.078
BP-cache	Arria 10	$256^3$	256	3.62	1.1	0.019
BP-prefetch	Arria 10	$256^3$	256	0.42	9.4	0.056

TABLE IV: Performance comparison of our work and other works

Our implementation could achieve better performance with more compute capability, so we plan to run the design on Intel Stratix 10 GX for future work. With the Stratix 10 device, we can express higher parallelism and achieve higher GUPS while using more DSPs.

#### V. CONCLUSION

We present in this paper an optimization based on back-projection algorithm for CT reconstruction using

FPGA BRAM efficiently. A reconstruction by blocks of voxels was developed to maximize data reuse and reduce external memory bandwidth, and maximize at the same time the use of the on-chip local memory. By expressing an higher computational intensity for 3D back-projection algorithm our design implementation performs 9.4 GUPS based on an efficient pipeline with no stall percentage on Intel Arria 10. Performances are therefore becoming closer to the ones obtained on embedded GPU. We plan to extend this work to the ray-driven projector to run a full iterative reconstruction, and also to further optimize the implementations to target the Intel Stratix device, which offers more computational capabilities.

## REFERENCES

- [1] F. B. Muslim *et al.*, “Efficient FPGA implementation of OpenCL high-performance computing applications via high-level synthesis,” in *IEEE Access*, vol. 5, 2017, pp. 2747–2762.
- [2] H. R. Zohouri *et al.*, “Evaluating and optimizing OpenCL kernels for high performance computing with FPGAs,” in *SC '16: Proceedings of the International Conference for High Performance Computing, Networking, Storage and Analysis*, 2016, pp. 409–420, ISSN: 2167-4337.
- [3] M. A. Mansoori *et al.*, “Efficient FPGA implementation of PCA algorithm for large data using hls,” in *PRIME Conference*, 2019.
- [4] E. Nurvitadhi *et al.*, “Can FPGAs beat GPUs in accelerating next-generation deep neural networks?” in *Proceedings of the 2017 ACM/SIGDA International Symposium on Field-Programmable Gate Arrays*, ser. FPGA '17. Association for Computing Machinery, 2017, pp. 5–14. <https://doi.org/10.1145/3020078.3021740>
- [5] S. Zhang *et al.*, “Research on OpenCL optimization for FPGA deep learning application,” in *PLoS ONE*, vol. 14, no. 10, 2019. <https://www.ncbi.nlm.nih.gov/pmc/articles/PMC6786543/>
- [6] “Intel stratix 10,” <https://www.intel.fr/content/www/fr/fr/products/programmable/fpga/stratix-10.html>.
- [7] “Intel agilex,” <https://www.intel.com/content/dam/www/programmable/us/en/pdfs/literature/wp/intel-agilex-fpgas-deliver-game-changing-com-bination-wp.pdf>.
- [8] N. Gac *et al.*, “High Speed 3D Tomography on CPU, GPU, and FPGA,” *EURASIP Emb Sys*, 2008.
- [9] F. Pfanner *et al.*, “High performance parallel backprojection on FPGA,” in *11th international meeting on Fully three-dimensional image reconstruction in radiology and nuclear medicine*, 2011. <https://www.osti.gov/etdeweb/biblio/22124816>
- [10] M. Leeser *et al.*, “Parallel-beam backprojection: an FPGA implementation optimized for medical imaging,” in *FPGA '02: Proceedings of the 2002 ACM/SIGDA tenth international symposium on Field-programmable gate arrays*, 2002, p. 25.
- [11] J. K. Kim *et al.*, “Forward-Projection Architecture for Fast Iterative Image Reconstruction in CT,” *IEEE Trans Sign Process*, 2012.
- [12] A. Cilardo, “Evaluating reconfigurable hardware for accelerating industrial CT,” in *2020 IEEE 7th International Conference on Industrial Engineering and Applications (ICIEA)*, 2020, pp. 93–97.
- [13] M. Ravi *et al.*, “FPGA as a hardware accelerator for computation intensive mlem medical image reconstruction,” *IEEE Access*, 2019.
- [14] D. Diakite *et al.*, “An OpenCL pipeline implementation on intel FPGA for 3D backprojection,” in *6th International Conference on Image Formation in X-Ray Computed Tomography*, 2020. <https://hal-centralesupelec.archives-ouvertes.fr/hal-02500994>
- [15] M. Martelli *et al.*, “3D Tomography back-projection parallelization on Intel FPGAs using OpenCL,” *Journal of Signal Processing Systems*, 2018. <https://hal.archives-ouvertes.fr/hal-01831884>
- [16] S. Wen *et al.*, “FPGA-accelerated automatic alignment for three-dimensional tomography,” in *2020 IEEE 28th Annual International Symposium on Field-Programmable Custom Computing Machines (FCCM)*, 2020, pp. 172–176, ISSN: 2576-2621.
- [17] Y.-k. Choi *et al.*, “Acceleration of EM-based 3D CT reconstruction using FPGA,” in *IEEE Transactions on Biomedical Circuits and Systems*, vol. 10, no. 3, 2016, pp. 754–767.
- [18] W. Zhang *et al.*, “FPGA acceleration for 3d low-dose tomographic reconstruction,” in *IEEE Transactions on Computer-Aided Design of Integrated Circuits and Systems*, 2020, pp. 1–1.
- [19] Intel, “Intel fpga sdk for opencl pro edition: Programming guide 2019,” .
- [20] M. A. Dávila-Guzmán *et al.*, “Analytical model of memory-bound applications compiled with high level synthesis,” in *2020 IEEE 28th Annual International Symposium on Field-Programmable Custom Computing Machines (FCCM)*, 2020. <http://arxiv.org/abs/2003.13054>
- [21] S. Williams *et al.*, “Roofline: an insightful visual performance model for multicore architectures,” in *Communications of the ACM*, vol. 52, no. 4, 2009, pp. 65–76. <https://dl.acm.org/doi/10.1145/1498765.1498785>
- [22] K. O. W. Group, “The opencl specification: Version 1.2,” <https://www.khronos.org/registry/OpenCL/specs/opencl-1.2.pdf>.
- [23] Y. Uguen *et al.*, “Application-specific arithmetic in high-level synthesis tools,” in *ACM Transactions on Architecture and Code Optimization*, 2019. <https://hal.archives-ouvertes.fr/hal-02423363>
- [24] K. Shata *et al.*, “Optimized implementation of OpenCL kernels on FPGAs,” in *Journal of Systems Architecture*, vol. 97, 2019, pp. 491–505. <http://www.sciencedirect.com/science/article/pii/S1383762118303151>
- [25] “Intel FPGA SDK for OpenCL pro edition: Best practices guide,” p. 193.
- [26] B. da Silva *et al.*, “Performance modeling for FPGAs: Extending the roofline model with high-level synthesis tools,” in *International Journal of Reconfigurable Computing*, 2013, Research Article. <https://www.hindawi.com/journals/ijrc/2013/428078/>
- [27] C.-Y. Chou *et al.*, “A fast forward projection using multithreads for multirays on GPUs in medical image reconstruction,” *Journal of Medical Physics Research and Practice*, 2011.